An experimental evaluation of the reliability of a damage localization algorithm based on FRF interpolation

Giorgio Busca[1] · Maria Pina Limongelli[2]

1 Introduction

The identification of structural damage before it gets irreversible or dangerous has gained a lot of attention among the research community in the last decades. Structural health monitoring by means of reliable and effective non-destructive damage identification techniques based on automatic measurement analysis will be the future of structural monitoring; traditional methods such as the visual inspection are often time consuming and sometimes not able to detect low levels of damage.

The damage identification process is based onto four main issues: the damage presence identification; the damage localization; the damage type qualification and the damage severity quantification [1, 2]. When all these four goals are achieved, the damage identification process can be considered done. The damage identification procedures described in literature are simple in terms of steps to be implemented, but the task is difficult to get by an automatic process, since there could be lot of practical limits, mainly due to the quality of the data and the way to get them. Damage configurations could depend upon several elements, such as the number of damage locations and their severity, but also the structure material and design, the environment conditions and most of all the quality of the measurement and signals processing.

Many damage identification algorithms are available in literature and most of them are based on the measurement of the structural vibrations eventually coupled to a proper mechanical modeling. Linear methods are very popular because they are based on simple assumptions: damage is a stiffness reduction, which modifies the structural dynamic parameters such as vibration frequencies [3–5], mode shapes and their curvatures [6–9] flexibility matrix [10–12], modal strain energy [13–15] and so on. The aim of

✉ Giorgio Busca
  giorgio.busca@polimi.it

  Maria Pina Limongelli
  mariapina.limongelli@polimi.it

[1] Department of Mechanical Engineering, Politecnico di Milano, Via La Masa 1, 20156 Milan, Italy

[2] Department of Architecture, Built Environment and Construction Engineering, Politecnico di Milano, Piazza Leonardo Da Vinci 32, 20133 Milan, Italy

these methods is the identification of one or more features, based on the dynamic parameters listed above, in order to define the presence of damage, its localization and its severity. Usually, damage is recognized by the comparison of these features between undamaged and damage scenarios. Several damage localization methods proposed in literature rely on modal curvatures as damage feature.

Another approach to damage identification that does not need the estimation of modal analysis is based on the definition of a damage index in terms of variations of the operational deformed shapes (ODSs) calculated from frequency response functions in the inspection phase with respect to a reference state. Abrupt changes of the ODS are interpreted as a symptom of a stiffness loss due to a localized damage. The Frequency Response Curvature Method (FRCM), proposed by Sampaio et al. [16], and the Gapped Smoothing Method (GSM), proposed by Ratcliffe [17], define a damage index in terms of the variation of curvature related to the reduction of stiffness and estimated from operational deformed shapes. More recently, Ramesh Babu and Sekhar [18] developed a technique for the localization of small cracks based on a damage detecting feature called slope deviation curve (SDC) calculated in terms of the slope of the operational deflection shapes.

The local reduction of smoothness in the curvature of the ODSs was proposed as a damage detecting feature also by Zhang et al. [19] in a new damage detection algorithm called Global Filtering Method (GFM) and based on the ODS extracted from the dynamic response of a passing vehicle excited by a sinusoidal tapping force. The drawback still connected with both these methods is that the numerical differentiation (needed to evaluate slope or curvature) introduces errors that often prevent the detection of damage in case of noisy data.

Methods based on the interpolation of the ODS using smooth functions to enhance the lack of smoothness at the location of damage do not require the estimation of curvature, thus overcoming some of the problems related to noise in recorded signals. Pai and Jin [20] proposed a boundary effect detection (BED) method based on the use of trigonometric functions to model the ODS of a beam and of a sliding window least-square curve fitting technique to estimate the coefficients of the curve. Based on the variations of values and sign of these coefficients along the beam, the location of damage can be detected.

Damage localization methods are sensitive to noise that may hamper the identification of the damage location in case of mild damage and a high noise-to-signal ratio. This problem affects most of the damage localization algorithms based on the analysis of the (modal or operational) deformed shapes, especially those based on the second derivative of the mode shapes in order to get the curvature.

The recently proposed Interpolation Damage Detection Method (IDDM) [21, 22] identifies the damage location as an incongruence between the cubic spline interpolation of the global deformed shape of the structure and the measured deformed shape and does not require numerical differentiation thus showing a lower sensitivity to noise in recorded data. A further advantage of the IDDM with respect to the method based on modal curvatures is that it gives a comparable level of accuracy without requiring the estimation of modal parameters. This property speeds up the damage identification process and potentially allows the implementation of an automatic damage localization system.

The method was tested on several cases such as a simulated damaged structure [22] and two damaged bridge ([21] and [23]), but was never applied using data from a bench test case under controlled boundary/environment conditions.

In this paper, the IDDM is applied using experimental data measured on three cantilever beams artificially damaged and subjected to hammer tests. The beams were damaged at specific locations and with controlled severity in order to simulate a known damage and thus verify the method damage sensitivity in several controlled configurations.

In order to verify the performance of the IDDM, results are compared to those given by the traditional Modal Shape Curvature Method (MSCM) proposed by Pandey [6] which is indeed a well-established procedure that is often used as benchmark to compare the performances of damage localization algorithms based on the analysis of feature related to the displacement profile of the structure.

Results show that the IDDM, requiring a lower computational effort with respect to the curvature method, gives a slightly higher level of accuracy in detecting the damaged region of a beam. Hence, it can be considered a good alternative, more feasible for automated damage localization, to well-known and consolidated methods of damage identification.

2 Methods for damage localization

2.1 The Interpolation Damage Detection Method (IDDM)

The IDDM is based on a damage feature defined as 'interpolation error' that quantifies the error connected with the approximation of the deformed profile of the structure by a cubic spline function. Specifically, the interpolation error is calculated at any given location as the difference between the vibrational amplitude actually measured and the vibrational amplitude computed at that same location

by interpolating the vibration amplitudes measured at all the other locations.

The possible increase of the interpolation error at one instrumented location between a reference state and an inspection state is assumed as indicator of the occurrence of structural damage close to the location where the change has been detected.

To make the paper self-contained, the basis of the IDDM is briefly recalled in the following. We refer to [21] and [22] for a more exhaustive presentation of the method.

It is assumed that the dynamic response of the beam is recorded by a network of sensors located along the longitudinal axes of the beam so that the vibrational profile, that is the experimental deformed shape of the beam, can be estimated through the frequency response functions (FRF) at all the instrumented locations.

The comparison between the smoothness of the operational deformed shapes (ODS) in the original and in the inspection phases gives information about the possible location of a reduction of stiffness: a sharp reduction of smoothness appears at a damaged location.

In order to enhance the difference between the smoothness of the ODSs in the reference and in the damaged configurations, a technique based on the cubic spline interpolation of the ODSs is applied.

At each location z along the longitudinal axes of the beam, the FRF is calculated interpolating through a cubic spline shape function the FRFs calculated form signals recorded at all the other instrumented locations (the dotted line in Fig. 1).

At the lth location z_l the FRF can be calculated through the spline interpolation using the following relationship:

$$H_S(z_l,f) = \sum_{j=0}^{3} c_{j,l}(f)(z_l - z_{l-1})^j,\tag{1}$$
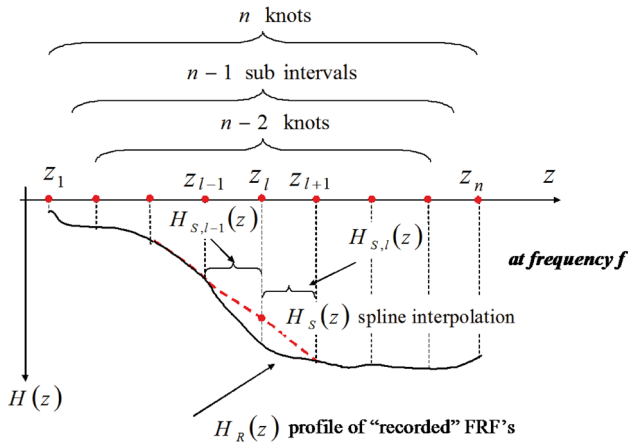
Fig. 1 Spline interpolation of the FRF at $z = z_l$

where the coefficients (c_{0l}, c_{1l}, c_{2l}, c_{3l}) are calculated from the values of the FRF "recorded" at the other locations:

$$c_{j,l}(f_i) = g(H_R(z_k,f_i)) \qquad k \neq l.\tag{2}$$

More details on the spline interpolation procedure can be found in Ref. [24].

The interpolation error at location z (in the following the index l will be dropped for clarity of notation) at the ith frequency value f_i, is defined as the magnitude of the difference between the recorded and interpolated FRFs:

$$E(z,f_i) = |H_R(z,f_i) - H_S(z,f_i)|,\tag{3}$$

where H_R is the FRF of the response recorded at location z and H_S is the spline interpolation of the FRF at z. In order to characterize each location with a single error parameter, the norm of the error on the whole range of frequencies has been considered:

$$E(z) = \sqrt{\sum_{i = n_0}^{n_0+N} E(z,f_i)^2}.\tag{4}$$

N is the number of frequency lines in the Fourier transform correspondening to the frequency range starting at line n_0, where the signal-to-noise ratio is high enough to allow a correct definition of the FRFs.

The values of the frequency response functions depend on the state of the structure hence if the estimation of the error function through Eq. (4) is repeated in the original and in the (potentially) damaged phases, the comparison between the two values, respectively, E_0 and E_d gives an indication about the existence of damage at the considered location.

$$\Delta E(z) = E_d(z) - E_0(z)\tag{5}$$

An increase in the interpolation error at a station between the reference configuration and the current configuration highlights a localized reduction of smoothness of the EDS and therefore a local variation of stiffness, associated with damage.

In order to remove the effect of random variations of the interpolation error E, that may lead to false detections of damage, a threshold value is defined so that a given location is considered damaged only if the variation ΔE of the interpolation error exceeds the threshold E_T.

If the distribution of the interpolation error in the undamaged configuration is available the threshold E_T can be calculated as the value corresponding to a given probability of exceedance in the undamaged configuration. If the structure is only occasionally tested to detect possible damages, as in the present case study, the available data at each instrumented location $\{z_l\}_{l=1}^{n}$ reduce to a single estimation of $E_0(z_l)$ and $E_d(z_l)$, for the undamaged and the possible

damaged structure, respectively, and the distribution of the interpolation error cannot be estimated. In this case, the lack of experimental data requires some simplifying assumptions. The assumption considered herein is that all sources of random variations equally affect all the instrumented locations producing a uniform variation (uniform increase or uniform decrease) of the interpolation error at all $\{z_l\}_{l=1}^n$ Based on this assumption, if a uniform variation of the interpolation error is detected, then the structure is considered undamaged and the possible variations of the interpolation error are ascribed to random sources not connected with damage. On the contrary, if the variation of the interpolation error ΔE is 'localized', namely it is 'significantly higher' at few locations with respect to the others, then a damage is denounced at those locations.

In order to select 'significant' values of ΔE, a threshold value must be introduced for this parameter in terms of its probability distribution. Assuming a normal distribution for ΔE, the threshold ΔE_{T} can be defined in terms of the average $\mu_{\Delta \mathrm{E}}$ and of the variance $\sigma_{\Delta E}$ of the damage parameter $\Delta E(z_l)$ on the population of available values (calculated at all the instrumented locations $\{z_l\}_{l=1}^n$), namely:

$$\Delta E_{\mathrm{T}} = \mu_{\Delta E} + v\sigma_{\Delta E}, \tag{6}$$

where v is the value of the standard normal distribution corresponding to the threshold probability.

If ΔE is normally distributed, then $v = 1$, $v = 2$, $v = 3$ lead to a confidence level of about 85, 98, 99 %, respectively, which means there is 15, 2, 1 % probability that $\Delta E(z_l)$ exceeds the threshold level in the undamaged configuration (false alarm).

A reduction of the fractile value, to which an increase of the threshold value of the damage index $\Delta(z_l)$ is associated, leads to a reduction of the false alarm risk but, at the same time, to an increased risk of "missed" alarms related to the possibility that also in the section actually damaged, the damage index does not exceed the threshold value. The choice of the minimum value of the damage index has to be the subject of a preliminary analysis, carried out on the structure to permit its determination on the basis of an acceptable compromise between the risk of having "false alarms" and of having "missed alarms".

For the application presented in this paper a value $v = 1$ has been assumed.

Once the threshold is estimated, the Interpolation Damage Index can be calculated at location z as the positive difference between the actual value of the interpolation error and the threshold:

$$\begin{aligned}
\mathrm{IDI}(z_l) =& \Delta E(z_l) - (\mu_{\Delta E} + v\sigma_{\Delta E}) \quad \text{if} \quad \Delta E(z_l) \\
& > (\mu_{\Delta E} + v\sigma_{\Delta E}) \qquad l = 1, \ldots, n \\
\mathrm{IDI}(z_l) =& 0 \quad \text{if} \quad \Delta E(z_l) < (\mu_{\Delta E} + v\sigma_{\Delta E})
\end{aligned} \tag{7}$$

2.2 Modal Shape Curvature Method (MSCM)

A method based on mode shape curvature was proposed for the first time by Pandey et al. [6], who stated that the damage location can be identified by the difference between the curvatures of a mode shape in the damaged and undamaged structure, respectively $\{\phi_{\mathrm{d}}''\}$ and $\{\phi''\}$:

$$\{\Delta\phi''\} = \{\phi_{\mathrm{d}}''\} - \{\phi''\} \tag{8}$$

Once the mode shapes Φ (undamaged) and Φ_{d} (damaged) are identified by means of a modal identification algorithm, the relevant curvature at a given location i on the structure can be estimated by a central difference method as:

$$\phi_i'' = (\phi_{i+1} - 2\phi_i + \phi_{i-1})/h^2, \tag{9}$$

where h is the distance between the measurement points $i + 1$ and i. The difference of the curvature mode shapes from intact and damaged structure can be a good indicator of damage location, as it was proved by literature. Recently Roy and Ray-Chaudhuri [25] demonstrated that the application of MSCM to spline-fitted mode shapes may lead to false damage detections if both positive and negative variations of curvature are considered. For this reason, only positive variations of the mode shape cur-vature have been considered herein as indications of the damage location. Moreover, in order to select the signif-icant value of the difference between the mode shape curvature (Eq. 8), a threshold like the one defined by Eq. (6) can be used. If the MSCM index is lower than the threshold $\mu_{\Delta\phi} + \sigma_{\Delta\phi}$, where $\mu_{\Delta\phi}$ is the average and $\sigma_{\Delta\phi}$ is the standard deviation of the MSCM values, the damage feature can be set to zero, otherwise it can keep its value. In this way, the statistical robustness of the damage detection should be ensured.

3 Description of the tests

3.1 Measurement setup

This section describes the experimental setup used to obtain the data needed to test the performance of the IDDM under controlled experimental conditions. The method was tested onto three cantilever beams of the same size. Nor-mally, experimental modal analysis on simple structures like beams should be performed in free–free boundary conditions, because tests in grounded conditions are very difficult to be implemented in practical case, since it is necessary to provide a foundation sufficiently rigid with respect to the structure [26]. However, structural health monitoring is usually applied to structures under working

conditions, where joints cannot be neglected. For this reason, a cantilever beam was chosen as test structure and the joint was properly designed to guarantee the required stiffness. The beams and the joint are shown in Fig. 2. Every beam was 750 mm long, it had a rectangular cross-section 30 × 10 mm and it was made of aluminum. Defects were simulated in terms of cross-section reduction, obtained by means of a thin blade saw, as shown in (Fig. 2c), where a 3-mm slot is visible on the 10-mm beam side.

The measurement setup involved 12 piezo-accelerometers PCB 333B30 with a 100 mV/g sensitivity, a 0.5–3.000 Hz frequency range and a ±50 g measurement range, equally displaced (one every 66 mm) along the axis of the beams, as shown in Fig. 3.

Since it was necessary to perform an experimental modal analysis, as it will be described in the following, the tests also required an impact hammer, in this case a PCB model 086C03 with a 2.25 mV/N sensitivity, a 0–8 kHz frequency range and a 2200 N measurement range. All the signals, properly filtered, were acquired with a 2000 Hz sample frequency by National Instruments hardware that guarantees the robustness of the acquisition in terms of signals synchronization and sampling time accuracy.

The tests were scheduled as described in the following. Each beam under undamaged conditions was excited along x direction (see Fig. 3a) by one impulse provided by the dynamometric hammer in correspondence of location 2 (see Fig. 3b). In the meantime, the acquisition hardware synchronously registered the signals from the dynamometric hammer and the accelerometers. The test was repeated 20 times for each beam, under undamaged conditions, in order to have 20 experimental transient responses for each sensor. Once 20 transient responses

were available for each accelerometer along the beam length, it was possible to estimate a frequency response function (FRF) between the force applied by the dynamometric hammer and the response recorded by each accelerometer. The function used to evaluate the FRF is the well-known H_1 estimator with a 0.05 Hz frequency resolution [26]. The noise of the transient response was properly reduced multiplying the signals by an exponential window. The FRFs were analyzed by means of a modal identification algorithm known as least squares complex exponential (LSCE) in order to estimate frequencies and normalized mode shapes, excited by the hammer [27].

After the dynamic characterization of the three cantilever beams in the undamaged conditions, a single progressive damage was imposed to each beam at three different locations along the z direction: one position for each beam (1/3L, 1/2L and 2/3L) where L is the beam length as shown in Fig. 3b. The damage was produced by a transversal slot with a rectangular section 2 mm width and three different depth levels, in order to simulate different damage severities, as shown in Fig. 2c and in table captions.

Table 1 describes the nine damage scenarios: three damage scenarios for each of the three beams.

The three damage levels imposed on the three beams correspond to a reduction of, respectively, 10, 20 and 30 % of the height of the cross-section. Each beam was tested in the undamaged and in each of the damaged configurations in order to calculate the FRFs and the modal parameters.
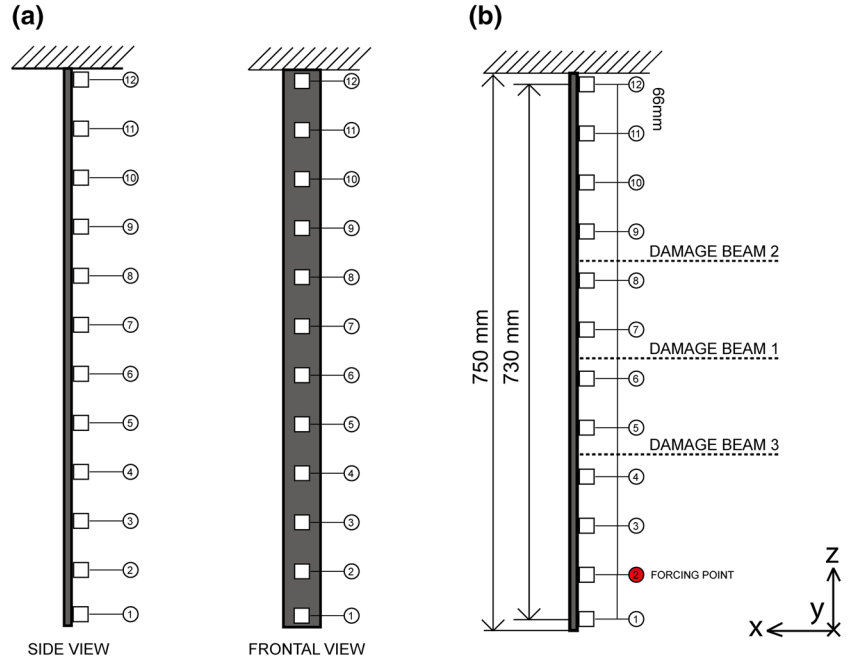
3.2 Data analysis

This section reports the results obtained in terms of frequency response function (FRF), modal frequencies and
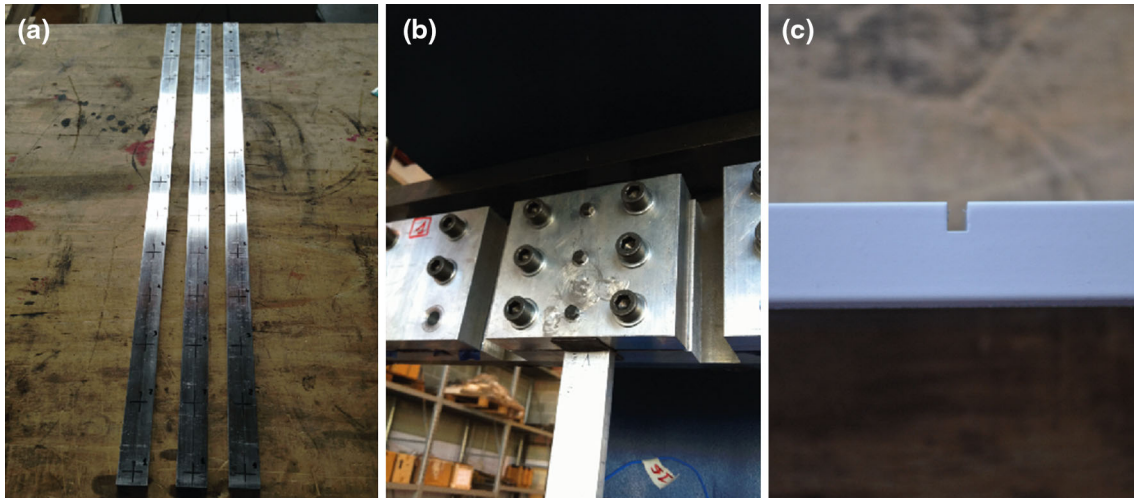
Fig. 2 **a** Beams; **b** joint design; **c** damage example

Fig. 3 Measurement setup

SIDE VIEW   FRONTAL VIEW

Table 1 Damaged configurations

BEAM	Damage location	Damage level
1	1/2 L = 375 mm between accelerometer 6 and 7	10 % = 1 mm slot depth
		20 % = 2 mm slot depth
		30 % = 3 mm slot depth
2	1/3 L = 250 mm between accelerometer 8 and 9	10 % = 1 mm slot depth
		20 % = 2 mm slot depth
		30 % = 3 mm slot depth
3	2/3 L = 500 mm between accelerometer 4 and 5	10 % = 1 mm slot depth
		20 % = 2 mm slot depth
		30 % = 3 mm slot depth

mode shapes. The FRFs of the undamaged beams obtained by the accelerometers are shown in Fig. 4 where three peaks are clearly visible in terms of [(m/s)^2/N] amplitude. The data are shown in the range 5–350 Hz where the values of the coherence function prove the correct detection of modes [26]. The FRFs were then used to apply the LSCE algorithm for the dynamic identification of modal parameters.
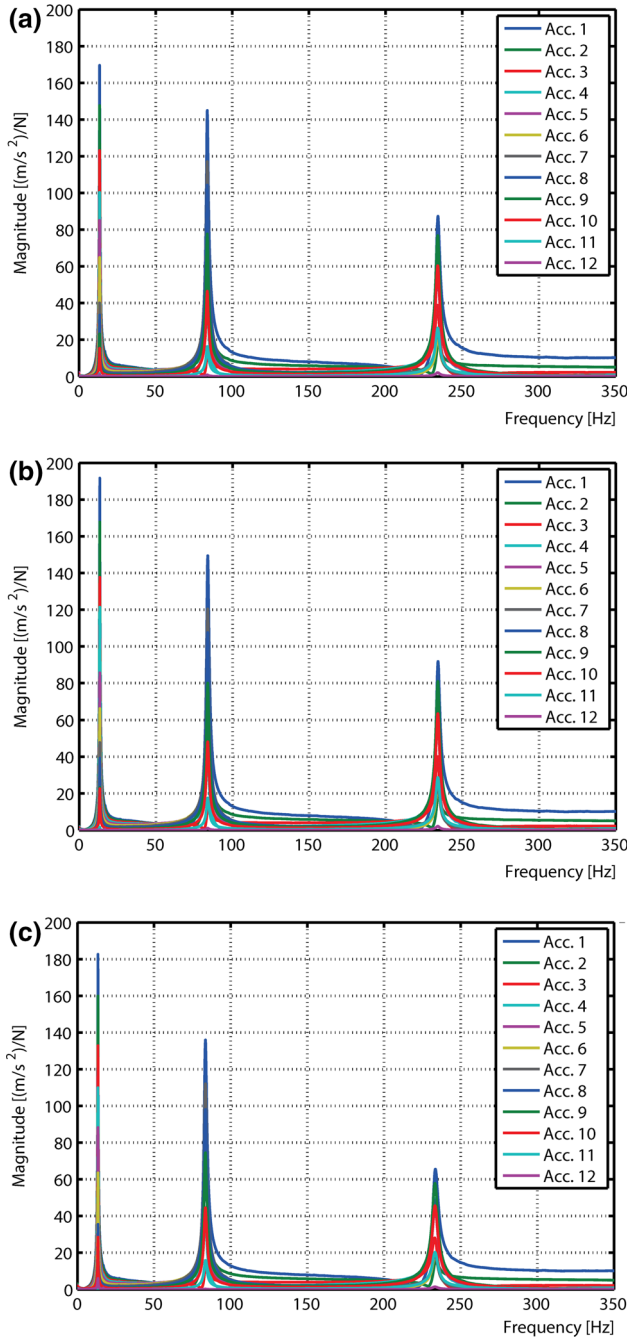
In order to quantify the severity of damage in terms of a parameter frequently used to detect global damage, the shifts of the first 3 modal frequencies with respect to the undamaged configuration are reported for each damaged scenario in Table 2.

As expected, having the same geometry and material, the three beams exhibit almost equal values of the modal frequency in the original configuration. At the increase of damage, modal frequencies decrease for many damage scenarios and the maximum shift, equal to 2.3 % of the original value, occurs for the 3rd mode of the 30 %

scenario of BEAM 3. This variation is quite small to be used as an effective damage indicator taking into account that, in a 'real world' case, due to the influence of experimental and ambient sources, such small variations would hardly be detected and furthermore cannot give information about the location of damage. For the tests presented herein the frequency variation is in many cases incompatible with the damage configuration, for instance the first frequency of BEAM 1 is steady for all the damage scenarios and the first frequency of BEAM 2 is higher in the scenario with 20 % of damage than in the undamaged configuration. These anomalies can be ascribed to a possible variation of the joint conditions which are difficult to be replicated for all the damage scenarios, even if the torque on the screws is controlled.

In the following sections, features related to the deformation of the beam (modal and operational shapes) will be used to localize damage.

Fig. 4 FRF amplitudes of the three cantilever beams at the measuring locations: **a** BEAM 1; **b** BEAM 2; **c** BEAM 3

Table 2 Identified modal frequencies and shifts for the undamaged and the damaged scenarios

	f_1 (Hz)	f_2	f_3	Δf_1 (%)	Δf_2 (%)	Δf_3 (%)
BEAM 1 (%)						
0	13.48	83.70	234.3			
10	13.43	83.55	233.8	0.4	0.2	0.2
20	13.43	83.48	234.3	0.4	0.3	0.0
30	13.43	82.58	234.0	0.4	1.3	0.1
BEAM 2 (%)						
0	13.45	83.90	234.1			
10	13.40	83.68	233.7	0.6	0.0	0.3
20	13.48	83.13	232.5	0.0	0.7	0.8
30	13.33	82.58	229.7	1.1	1.3	2.0
BEAM 3 (%)						
0	13.40	83.58	233.6			
10	13.35	83.43	233.3	1.0	0.3	0.4
20	13.45	82.48	230.4	0.2	1.5	1.7
30	13.45	82.1	228.9	0.2	1.9	2.3

observed also for the modal shapes relevant to BEAM 2 and BEAM 3, similar to that of BEAM 1. The source of these irregularities could be found in the choice of the sensors. Probably the sensor sensitivity was too much low to get correctly the vibrations of the half part of the beam near the joint, where the vibration levels are small for the first bending mode. This is quite evident if the FRFs rele-vant to points 6–12 are analyzed (see Fig. 6). They show that the contribution of the first mode to the accelerations recorded near the joint (points 6–12) is lower than the contribution of the second and the third modes, hence is likely to be much more affected by the low sensitivity of the sensors with respect to the contributions of the other two modes. However, it must be noticed that the coherence function of all the channels was higher than 0.95 in cor-respondence of the first mode.

Since the identification of the first mode was clearly ambiguous for all the beams and the reason of this situation is not verified, in the following, the damage identification will be carried out based on data relevant to the second and the third mode that, in reverse, show a clear variation due to damage.

It is noted that in a real case the removal of the unre-liable data would not be possible since the exact location of damage would not be known a priori. Herein the removal of the data relevant to the first mode was carried out just to check the performance of the damage identification algo-rithms based on good experimental data and to shown the difference between using reliable and unreliable recorded data.

As shown by Fig. 5, the second mode shows an alter-ation of its shape in the area close to the location of damage

The first three bending mode shapes of the BEAM 1 are reported in Fig. 5 for the undamaged condition and for the three damaged scenarios. It can be seen that the first modal shape exhibits some irregularities at locations 6–12 that are incongruent with a smooth first bending mode of an undamaged cantilever beam with constant section along its axis. Furthermore, it is noted that this effect is present only on the first mode, whereas the shapes of the other two modes appear smooth at the same locations. This trend is

Fig. 5 Bending mode shapes of beam 1 in the three damage scenarios: **a** mode 1; **b** mode 2; **c** mode 3

(black dotted line), whereas the third mode shows a variation at locations 5 and 9. In the damaged configurations the mode shapes show changes not clearly related to the damage location (only mode 2 shows a clear change at the damage location). Similar considerations can be drawn for the other two damage scenarios, thus confirming the poor sensitivity of modal shapes to damage, widely discussed in literature [1, 28, 29].
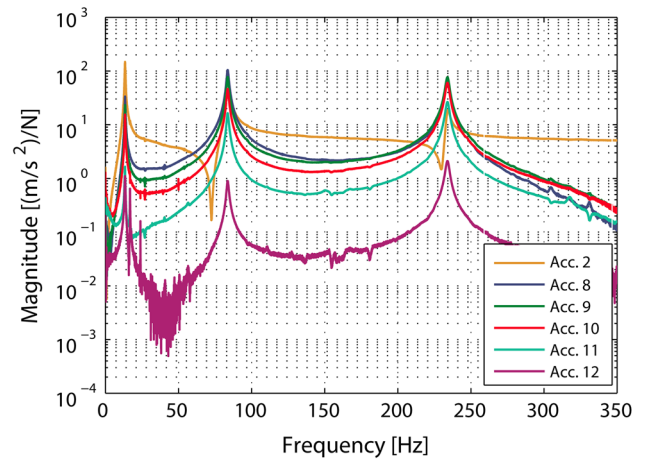
Fig. 6 FRF amplitudes at the hitting point 2 and at nodes close to the joint

4 Results

4.1 Application of the MSCM

Figure 7 shows the variation of curvatures estimated for the second and third mode in all the damaged scenarios listed in Table 1.

Curvatures are estimated at locations 2–11 by applying Eq. (9) after a spline fitting of the mode shapes. At locations 1 and 12 the values of curvature cannot be estimated via Eq. (9) hence the curvature variation is not considered at these two locations.

The black point specifies the actual location of damage on the beam.

Based on results relevant to the second and/or third modal curvatures, the MSCM damage index reaches the maximum value at locations close to the damage position almost for all the damage scenarios (only the positive values of the index were considered). This point out the robustness of the procedure improved by the redundancy related to the availability of one value of the damage index for each mode.

The comparison between the values of the MSCM damage index relevant to the two modes shows that the indexes estimated basing on the second mode data are the most consistent. The damage is always identified for all the beams in every damage scenario except for damage scenario 1 mm for BEAM3.

The values of the MSCM damage index relevant to the third mode are less sensitive to low levels of damage (10 %) but allow a reliable detection for damages of medium to high severity (20, 30 %).

For all the specimens some false alarms are given, both for low and for high severity of damage, if results relevant
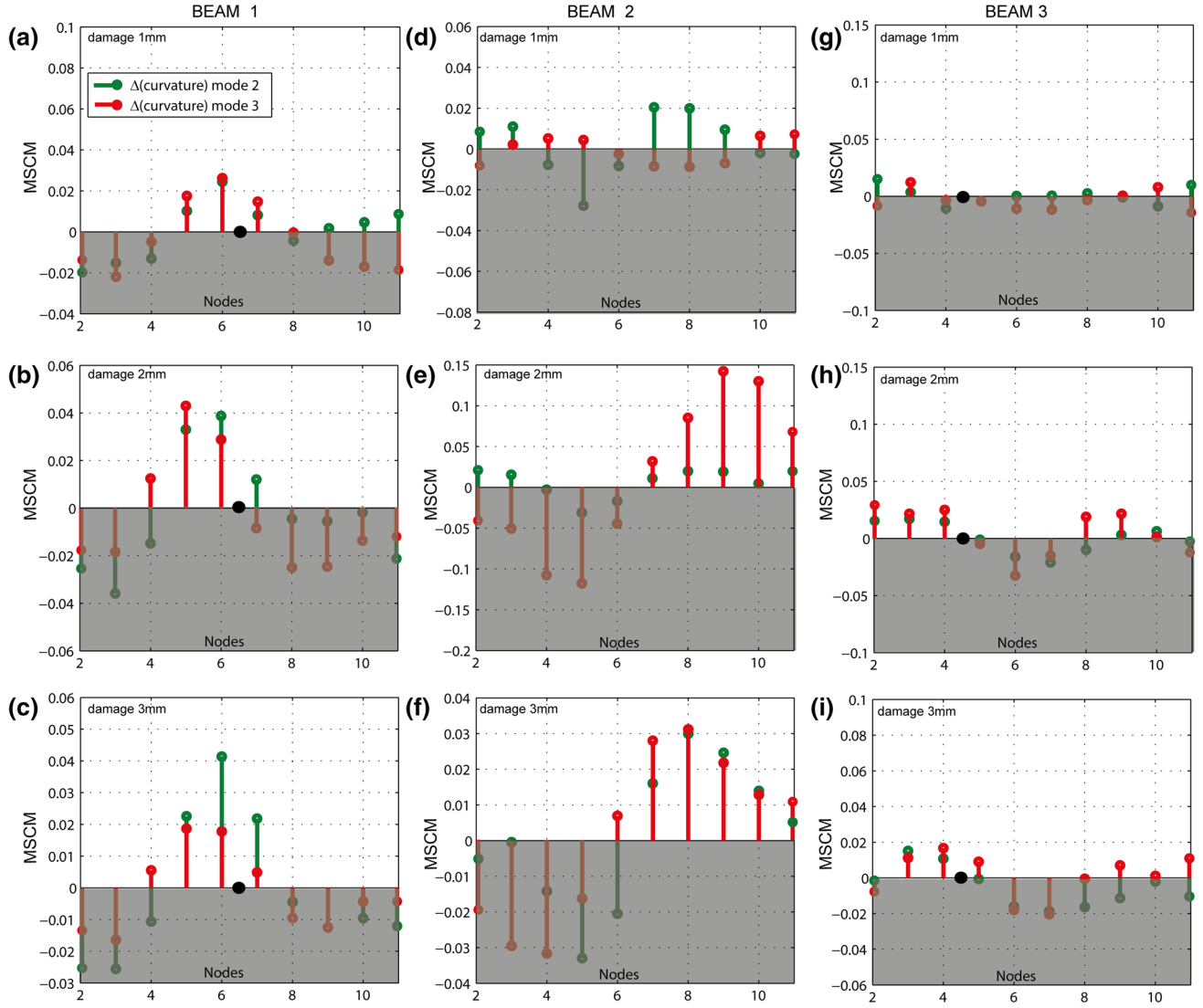
Fig. 7 Curvature damage index: **a** beam 1 damage 1 mm; **b** beam 1 damage 2 mm, **c** beam 1 damage 3 mm; **d** beam 2 damage 1 mm; **e** beam 2 damage 2 mm; **f** beam 2 damage 3 mm; **g** beam 3 damage 1 mm; **h** beam 3 damage 2 mm; **i** beam 3 damage 3 mm

to the third mode are considered; for instance in BEAM 3 with 20 % of damage there is a false positive at locations 8 and 9. If a threshold is used, as the one used for the IDDM method (Eq. 6), the damage index values are normalized on their statistical distribution, but this operation is inef-fective in order to filter out some false alarms. Indeed, the data in Fig. 8 shows the damage index after the thresh-olding and, in most of the cases, false alarms are still present.

4.2 Application of the IDDM

Results of the application of the Interpolation Method are reported in Figs. 9, 10, 11 in terms of the variation of the Interpolation Error (ΔE) defined by Eq. (5) and in terms of the Interpolation Damage Index (IDI), defined by

Eq. (7). The interpolation error is calculated according to Eq. (4) in the frequency range (50–260 Hz) including the second and the third modes of vibrations. The actual location of damage is shown by a dashed black vertical line.

For the case of BEAM1, reported in Fig. 9, damage is correctly identified for all the scenarios as located around location 6 and 7. For damage level 1 mm, a false alarm is found around location 9 but the value of the damage index at this location is quite lower than the values close to the actually damaged section thus is relatively straightforward to detect the actual damaged location.

For BEAM 2, as shown in Fig. 10, the correct location of damage (between nodes 8 and 9) is detected for all levels of damage severity. No false alarms are reported in this case.
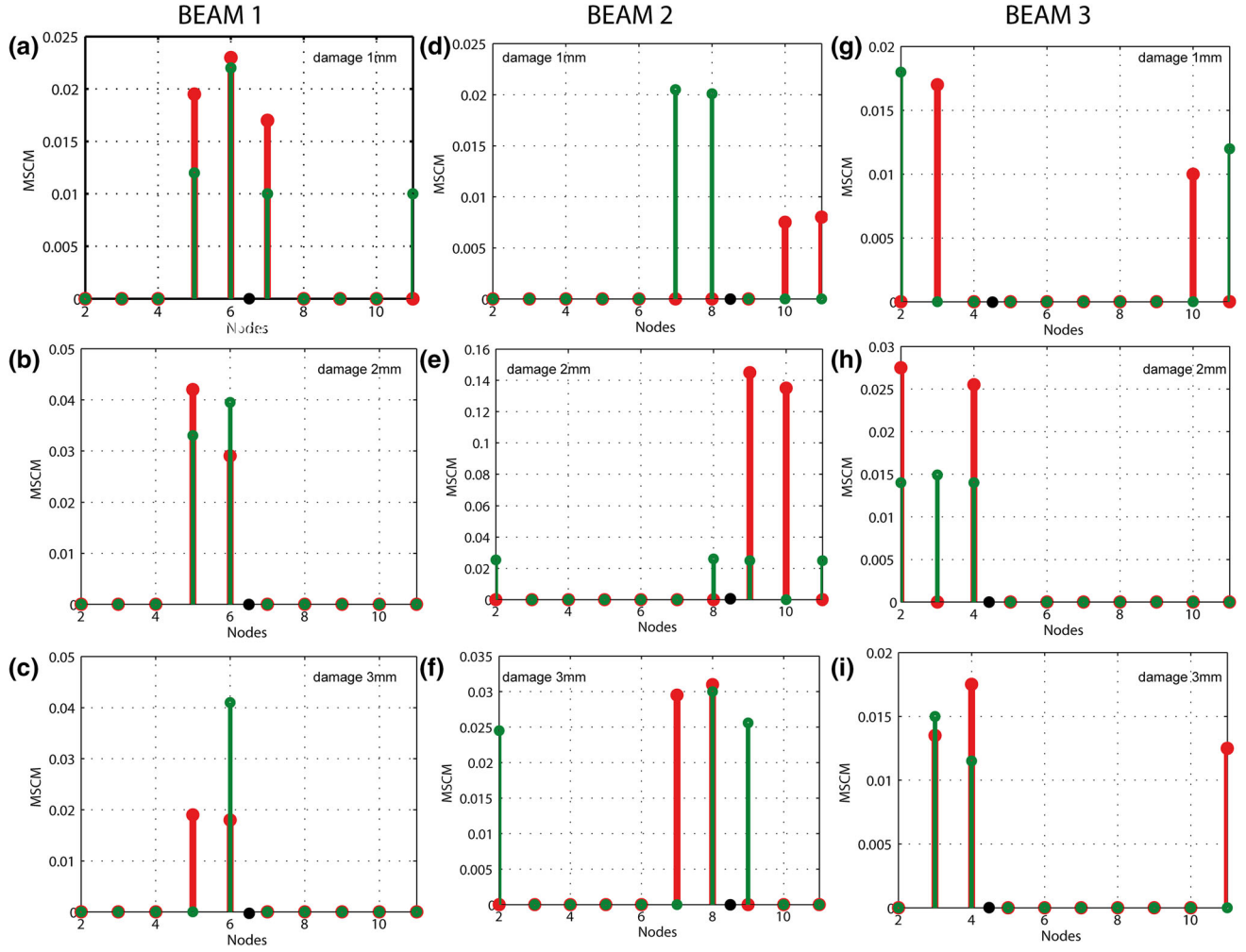
Fig. 8 Curvature damage index after thresholding: **a** beam 1 damage 1 mm; **b** beam 1 damage 2 mm; **c** beam 1 damage 3 mm; **d** beam 2 damage 1 mm; **e** beam 2 damage 2 mm; **f** beam 2 damage 3 mm; **g** beam 3 damage 1 mm; **h** beam 3 damage 2 mm; **i** beam 3 damage 3 mm
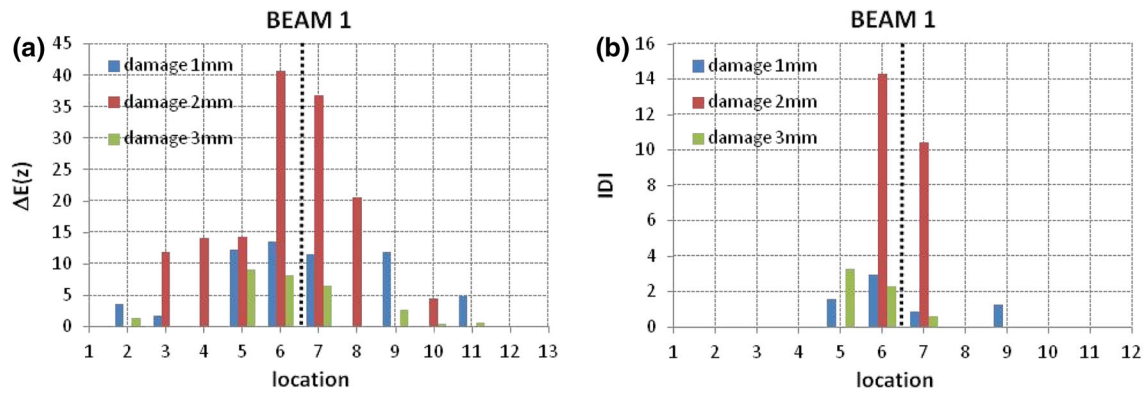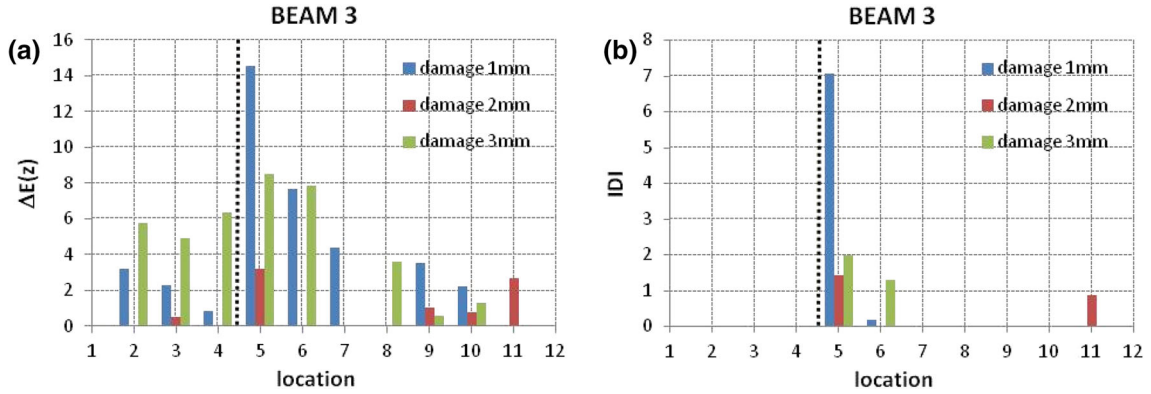

Fig. 9 Results of damage localization via IDDM for BEAM 1. Frequency range (50–260 Hz)

Also for the case of BEAM 3 (Fig. 11), damage is correctly identified for damage levels 1 and 3 mm, but there is a false alarm at location 11 for level 2 mm.

It is noted that the false alarms, both for BEAM1 and for BEAM 3 are found in the region where, as reported in Sect. 3.2, the sensor sensitivity was probably too much low to get correctly the vibrations of the beam.
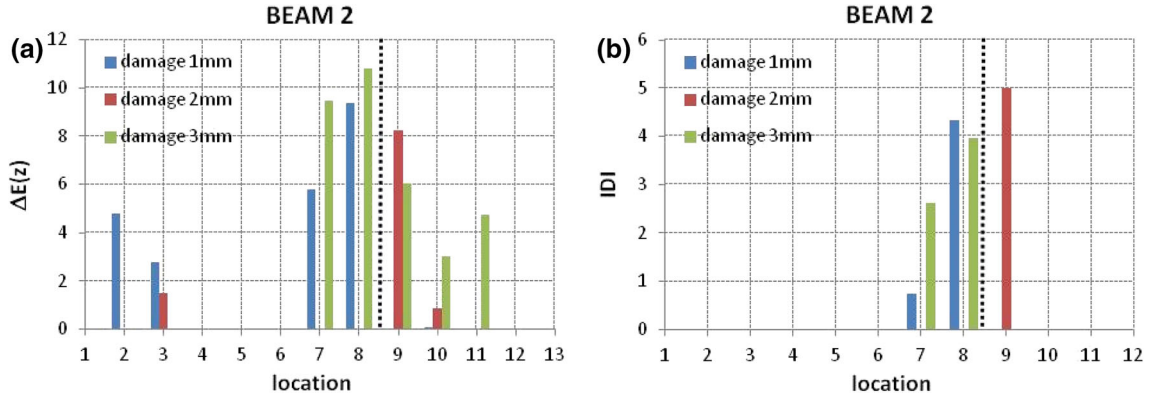
Fig. 10 Results of damage localization via IDDM for BEAM 2. Frequency range (50–260 Hz)
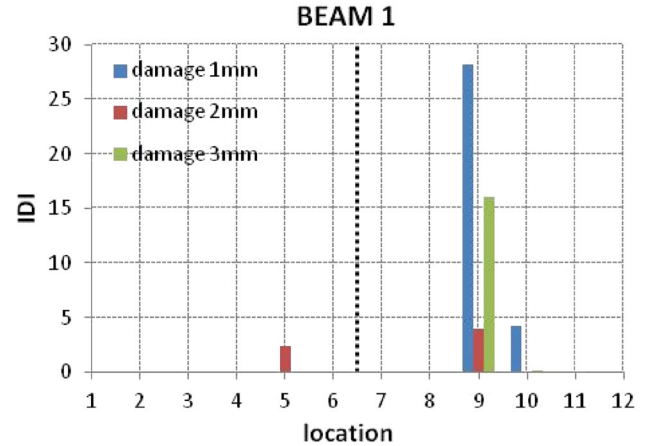

Fig. 11 Results of damage localization via IDDM for BEAM 3. Frequency range (50–260 Hz)

In order to compare these results to those given by applying the IDDM to unreliable data, in Fig. 12 are reported results obtained for BEAM 1 by applying the IDDM to the whole frequency range between 10 and 260 Hz. The algorithm finds a damage in the region corresponding to locations 9 and 10. This is consistent with the irregularity of the first modal shape pointed out in Sect. 3.2, but it is of course misleading for detecting the real damage located between nodes 6 and 7.

As general comment, as for all damage localization algorithms based on deformed shapes, the IDDM is able to detect correctly the damaged portion of the beam, provided reliable experimental data are available.

4.3 Comments

The performances of both the methods MSCM and IDDM depend on the number of sensors deployed on the structure and on the quality of their signal. Since MSCM needs to estimate the mode shape curvatures, the sensors have to be placed in the correct position to avoid spatial aliasing. For the experimental case presented in this paper, the amount of sensor is close to the minimum requirement to correctly

Fig. 12 Results of damage localization via IDDM for BEAM 1. Frequency range (10–260 Hz)

estimate the third bending mode. Moreover, Sazonov and Klinkhachorn [30] verified that a correlation exists between the amount of noise on the signals and the spatial resolution of the measurement mesh. Increasing the number of sensors has a positive effect on the spatial accuracy of damage detection, but the negative influence of noise is more

important because of the discrete derivative process to obtain the curvature. This happens because the second-order discrete difference of the mode shape is a really sensible to noise if the measurement points are close to each other.

The IDDM can obviously benefit from a high spatial resolution of the sensors allowing a better description of the operational deformed shapes, hence a more reliable estimation of the damage index. On the other hand, the IDDM does not require the estimation of the curvatures (hence of the second derivatives of the ODSs); hence, for a given pattern of recording sensors, it is less affected by noise in recorded data with respect to the MCSM.

The results discussed in Sects. 4.1 and 4.2 show the effectiveness of both the methods, which are both capable of detecting the damage. However, the IDDM seems to be more reliable, since the use of the threshold allows filtering out almost all the false alarms. For instance, Fig. 8d displays the damage index obtained by the MSCM method for BEAM 2 and 1 mm damage.

Even though a threshold is used also with this method, two false alarms at positions 10 and 11 are detected. The same damage scenario is correctly identified by the IDDM method removing the false damage positions (see Fig. 10b). Same considerations can be inferred for all damage scenarios of BEAM 3, where several false alarms are given by MSCM while for IDDM there is just one false alarm for damage 2 mm (see Fig. 11b).

5 Conclusions

In this paper, the comparison between the Interpolation Damage Detection Method (IDDM) and the Modal Shape Curvature Method (MSCM) has been achieved through experimental data coming from a bench test structure.

Experimental data were obtained by three cantilever aluminum beams for which several different damage scenarios were artificially reproduced in laboratory. Frequency response functions were calculated at several locations along the beams axis through impact hammer testing and used to localize the damage location via the IDDM and via the more traditional MSCM.

Results show that both method of damage detection are influenced by the inaccuracies in recorded data that hamper the damage localization. Furthermore, both the MSCM and the IDDM exhibit a certain degree of robustness given by the possibility of evaluating the damage index with reference to different modal contributions (for the MCSM) or frequency ranges (for the IDDM).

Finally, the comparison of results given by the two methods shows that, despite the lower computational burden, damage localization via the IDDM gives the same rate of success in terms of correct damage localization as the MSCM, but the number of false alarms (wrong detection of damage at location that are actually intact) is lower if the IDDM is applied.

References

1. Carden EP (2004) Vibration based condition monitoring: a review. Struct Heal Monit 3:355–377
2. Farrar C, Jauregui D (1999) Comparative study of damage identification algorithms applied to a bridge: I. Experiment. Smart Mater Struct 7:704
3. Salawu OS (1997) Detection of structural damage through changes in frequency: a review. Eng Struct 19:718–723
4. Patil DP, Maiti SK (2003) Detection of multiple cracks using frequency measurements. Eng Fract Mech 70:1553–1572
5. Yang Z, Wang L (2009) Structural damage detection by changes in natural frequencies. J Intell Mater Syst Struct 21:309–319
6. Pandey A, Biswas M, Samman M (1991) Damage detection from changes in curvature mode shapes. J Sound Vib 145:321–332
7. Ratcliffe C (2000) A frequency and curvature based experimental method for locating damage in structures. J Vib Acoust 122:324–329
8. Hamey CS (2004) Experimental damage identification of carbon/epoxy composite beams using curvature mode shapes. Struct Heal Monit 3:333–353
9. Yoon M-K, Heider D, Gillespie JW, Ratcliffe CP, Crane RM (2009) Local damage detection with the global fitting method using mode shape data in notched beams. J Nondestruct Eval 28:63–74
10. Li G, Hao K, Lu Y, Chen S (1999) A flexibility approach for damage identification of cantilever-type structures with bending and shear deformation. Comput Struct 73:565
11. Zhou Z, Wegner L, Sparling B (2007) Vibration-based detection of small-scale damage on a bridge deck. J Struct Eng 133:1257–1267
12. Li J, Wu B, Zeng QC, Lim CW (2010) A generalized flexibility matrix based approach for structural damage detection. J Sound Vib 329:4583–4587
13. Shi Z, Law S, Zhang L (1998) Structural damage localization from modal strain energy change. J Sound Vib 218:825–844
14. Kim J-T, Stubbs N (2002) Improved damage identification method based on modal information. J Sound Vib 252:223–238
15. Choi S, Park S, Park N-H, Stubbs N (2006) Improved fault quantification for a plate structure. J Sound Vib 297:865–879
16. Sampaio R, Maia N, Silva J (1999) Damage detection using the frequency-response-function curvature method. J Sound Vib 226:1029–1042
17. Ratcliffe CP (1997) Damage detection using a modified laplacian operator on mode shape data. J Sound Vib 204:505–517
18. Ramesh Babu T, Sekhar AS (2008) Detection of two cracks in a rotor-bearing system using amplitude deviation curve. J Sound Vib 314:457–464
19. Zhang Y, Lie ST, Xiang Z (2013) Damage detection method based on operating deflection shape curvature extracted from dynamic response of a passing vehicle. Mech Syst Signal Process 35:238–254
20. Pai PF, Jin S (2000) Locating structural damage by detecting boundary effects. J Sound Vib 231:1079–1110
21. Limongelli MP (2010) Frequency response function interpolation for damage detection under changing environment. Mech Syst Signal Process 24:2898–2913

22. Limongelli MP (2011) The interpolation damage detection method for frames under seismic excitation. J Sound Vib 330:5474–5489
23. Limongelli MP (2014) Seismic health monitoring of an instrumented multistorey building using the Interpolation Method. Earthq Eng Struct Dyn 43:1581
24. Limongelli MP (2003) Optimal location of sensors for reconstruction of seismic responses through spline function interpolation. Earthq Eng Struct Dyn 32:1055–1074
25. Roy K, Ray-Chaudhuri S (2013) Fundamental mode shape and its derivatives in structural damage localization. J Sound Vib 332:5584–5593
26. Ewins DJ (2010) Modal testing: theory, practice and application (Mechanical Engineering Research Studies: Engineering Dynamics Series). Wiley, New York
27. Maia NMM, Silva JMM e (1997) Theoretical and experimental modal analysis (Mechanical Engineering Research Studies. Engineering Control Series, 9). p 488
28. Alvandi A, Cremona C (2006) Assessment of vibration-based damage identification techniques. J Sound Vib 292:179–202
29. Fan W, Qiao P (2010) Vibration-based damage identification methods: a review and comparative study. Struct Heal Monit 10:83–111
30. Sazonov E, Klinkhachorn P (2005) Optimal spatial sampling interval for damage detection by curvature or strain energy mode shapes. J Sound Vib 285:783–801